A Comparative Study of Pressure-Dependent Emission Characteristics in Different Gas Plasmas Induced by Nanosecond and Picosecond Neodymium-Doped Yttrium Aluminum Garnet (Nd:YAG) Lasers

Syahrun Nur Abdulmadjid,[a] Nasrullah Idris,[a] Alion Mangasi Marpaung,[b] Marincan Pardede,[c] Eric Jobiliong,[d] Rinda Hedwig,[e] Maria Margaretha Suliyanti,[f] Muliadi Ramli,[g] Heri Suyanto,[h] Kiichiro Kagawa,[i] May On Tjia,[j,k] Zener Sukra Lie,[j] Tjung Jie Lie,[j] Hendrik Koo Kurniawan[j]*

[a] *Department of Physics, Faculty of Mathematics and Natural Sciences, Syiah Kuala University, Darussalam, Banda Aceh 23111, NAD, Indonesia*
[b] *Department of Physics, Faculty of Mathematics and Natural Sciences, Jakarta State University, Rawamangun, Jakarta 12440, Indonesia*
[c] *Department of Electrical Engineering, University of Pelita Harapan, 1100 M.H. Thamrin Boulevard, Lippo Village, Tangerang 15811, Indonesia*
[d] *Department of Industrial Engineering, University of Pelita Harapan, 1100 M.H. Thamrin Boulevard, Lippo Village, Tangerang 15811, Indonesia*
[e] *Department of Computer Engineering, Bina Nusantara University, 9 K.H. Syahdan, Jakarta 14810, Indonesia*
[f] *Research Center for Physics, Indonesian Institute of Sciences, Kawasan PUSPIPTEK, Serpong, Tangerang Selatan 15314, Banten, Indonesia*
[g] *Department of Chemistry, Faculty of Mathematics and Natural Sciences, Syiah Kuala University, Darussalam, Banda Aceh 23111, NAD, Indonesia*
[h] *Department of Physics, Faculty of Mathematics and Natural Sciences, Udayana University, Kampus Bukit Jimbaran, Denpasar 80361, Bali, Indonesia*
[i] *Research Institute of Nuclear Engineering, University of Fukui, Fukui 910-8507, Japan*
[j] *Research Center of Maju Makmur Mandiri Foundation, 40 Srengseng Raya, Kembangan, Jakarta Barat 11630, Indonesia*
[k] *Physics of Magnetism and Photonics Group, Faculty of Mathematics and Natural Sciences, Bandung Institute of Technology, 10 Ganesha, Bandung 40132, Indonesia*

An experimental study has been performed on the pressure-dependent plasma emission intensities in Ar, He, and N_2 surrounding gases with the plasma induced by either nanosecond (ns) or picosecond (ps) yttrium aluminum garnet laser. The study focused on emission lines of light elements such as H, C, O, and a moderately heavy element of Ca from an agate target. The result shows widely different pressure effects among the different emission lines, which further vary with the surrounding gases used and also with the different ablation laser employed. It was found that most of the maximum emission intensities can be achieved in Ar gas plasma generated by ps laser at low gas pressure of around 5 Torr. This experimental condition is particularly useful for spectrochemical analysis of light elements such as H, C, and O, which are known to suffer from intensity diminution at higher gas pressures. Further measurements of the spatial distribution and time profiles of the emission intensities of H I 656.2 nm and Ca II 396.8 nm reveal the similar role of shock wave excitation for the emission in both ns and ps laser-induced plasmas, while an additional early spike is observed in the plasma generated by the ps laser. The suggested preference of Ar surrounding gas and ps laser was further demonstrated by outperforming the ns laser in their applications to depth profiling of the H emission intensity and offering the prospect for the development of three-dimensional analysis of a light element such as H and C.

Index Headings: **Picosecond YAG laser; Low pressure plasma; Shock wave; Hydrogen analysis; Light element; Laser-induced breakdown spectroscopy; LIBS.**

INTRODUCTION

Laser-induced plasma spectroscopy (LIPS) for spectrochemical analysis has been an active field of study since the first demonstration made by Brech and Cross in 1962.[1] Further development of this method was proposed by Radziemski et al.,[2] in which the laser-target interaction takes place in an atmospheric-pressure surrounding gas and is now commonly referred to as laser-induced breakdown spectroscopy (LIBS). In this technique, a laser pulse of several tens of millijoules is focused on the sample resulting in a high-temperature and high-density plasma. A gated optical multichannel analyzer (OMA) was used to remove the initial strong background emission of the plasma. Researchers are drawn to the simplicity of generating the laser-induced plasma and a number of unique advantages offered by this technique. Apart from eliminating the need for tedious sample preparation, spectrum measurement can be carried out without sample transport. This method also allows for the implementation of local microanalysis[3–9] and offers the feasibility of obtaining real-time, online analytical information.[10] This method is enjoying a growing range of applications thanks to the rapid development of ablation lasers[11–15] and the continued improvement of its sensitivity and accuracy.[16–20] Its advantages have been amply demonstrated in rapid quantitative analysis in various fields such as cultural heritage applications,[21–24] industrial applications,[25–30] environmental contamination studies,[31–35] biomedical applications,[36–40] and aerosols analysis.[41–45] However, relatively little has been reported on the application of LIBS dedicated to the important analysis of hydrogen and carbon in solid samples for reasons explained in the following.

Received 10 December 2012; accepted 21 June 2013.
* Author to whom correspondence should be sent. E-mail: kurnia18@cbn.net.id.
DOI: 10.1366/12-06952

0003-7028/13/6711-1285/0

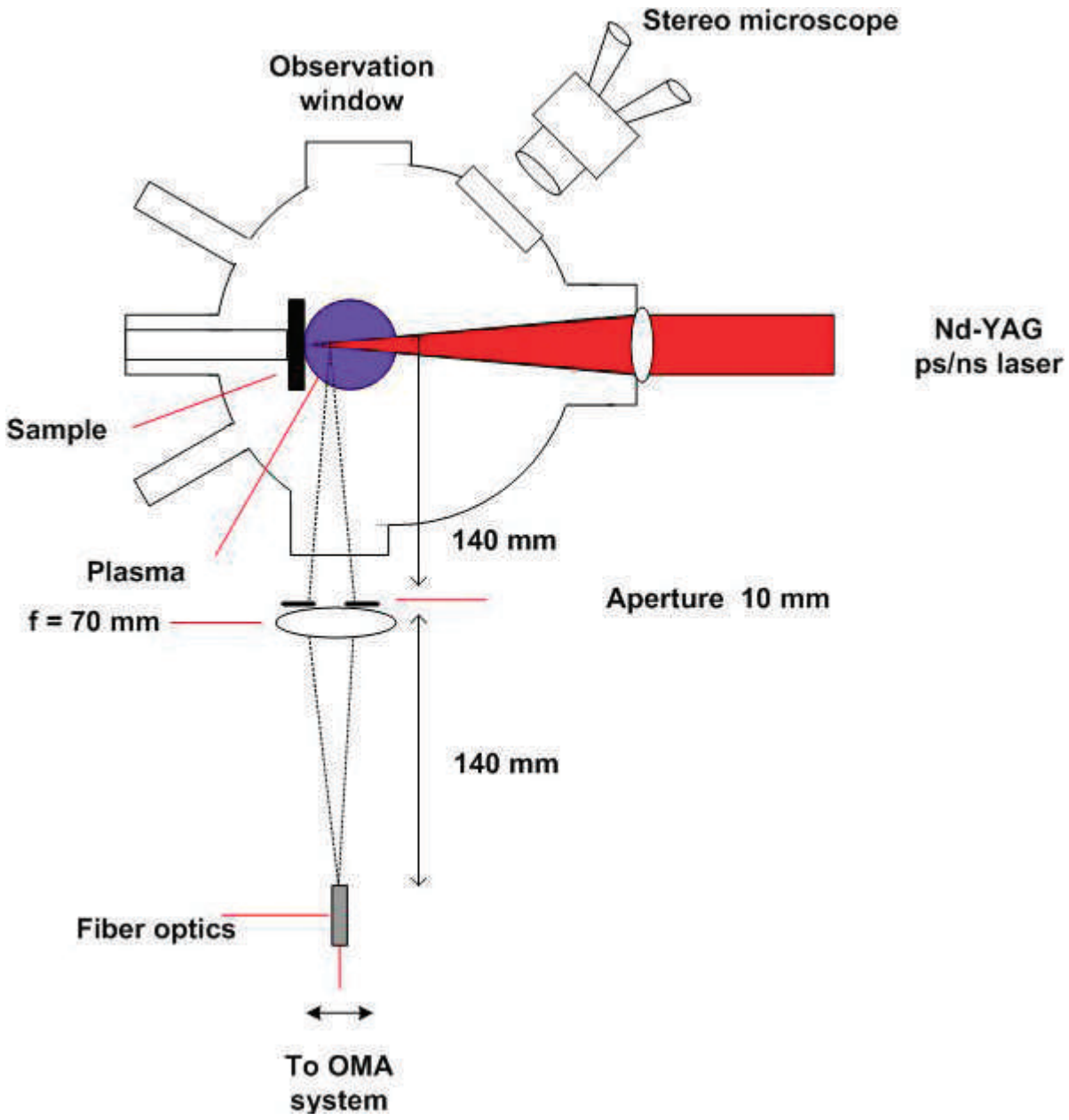

FIG. 1. Diagram of the experimental setup.

Firstly, a high-density plasma produced in LIBS generally contains a large number of charged particles that produce a strong internal electric field. As a consequence, emission lines from the ablated atoms invariably suffer from the Stark broadening effect, which is particularly severe in the case of hydrogen atom.[46,47] Secondly, an important reason for the difficulty of hydrogen analysis in conventional LIBS is the drastic reduction of hydrogen emission with increased ambient gas pressure, resulting in very weak intensity at 1 atm.[48–49] This seemingly anomalous behavior is satisfactorily explained within the framework of the shock wave excitation model as a consequence of time mismatch between the fast passage of the relatively light hydrogen atoms and the formation of the shock wave, which is induced mainly by the heavier atoms of the solid target. Therefore, most of the hydrogen atoms are expected to miss the shock wave excitations process. This time mismatch is known to become more detrimental at higher gas pressure,[48–49] leading to failure of LIBS for hydrogen analysis of solid samples.

In a series of experiments, we successfully detected the strong and sharp H I 656.2 nm emission line from solid samples of zircaloy plate with low-pressure surrounding gas.[49,50] The resulting calibration curve clearly indicates the potential use of this technique for quantitative analysis. Similar excellent results were also obtained for H and C emission lines from solid organic samples and geological samples employing low-pressure plasma.[51] Unfortunately, this result was achieved at the cost of leaving sizeable craters of roughly 0.4 mm diameter on the sample surfaces, which renders the technique unsuitable for microanalysis. Thus, for the extension of its applicability, the resulting crater size must be reduced. In addition to that, depth profiling of the element distribution inside the sample is also much desired for providing information of three-dimensional distribution of the elements

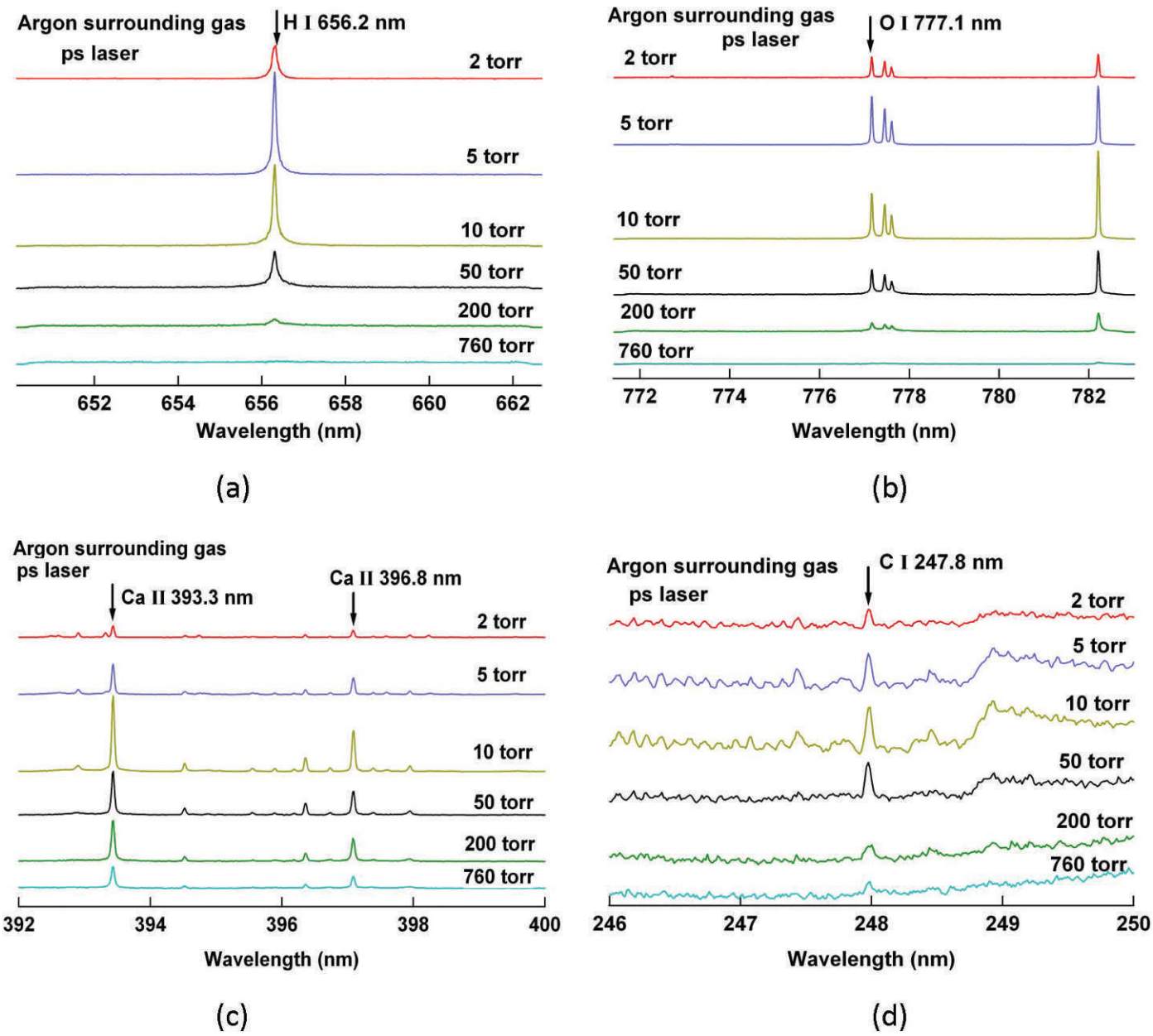

FIG. 2. Spatial and time-integrated emission spectrum of (**a**) hydrogen, (**b**) oxygen, (**c**) calcium, and (**d**) carbon in various surrounding argon gas pressure when picosecond laser of energy 7 mJ was used for ablation of agate sample.

of interest in the sample. So far, experiments on depth profile measurement of H impurity have neither been performed in our previous works nor published by different groups in the literature.

It is therefore the purpose of the current study to address those two issues and to propose their appropriate solutions. For that purpose, a picosecond Neodymium-doped yttrium aluminum garnet (ps Nd:YAG) laser was employed in this experiment for the study of its comparative merits with respect to the existing common use of a nanosecond (ns) laser. Additionally, the relative advantages of different surrounding gases, namely Ar, N_2, and He gases were also investigated for this study. The target used for the study was an agate sample (composition: 28.2% calcium, 12.7% aluminum, 13.2% silica, 0.9% hydrogen, 3% carbon, and 42% oxygen), where the light elements such as H, C, N, O, and a heavy element such as Ca are known to have relatively high concentrations with homogeneous distribution in the sample. It is therefore suitable for exhibiting and distinguishing the different pressure-dependent variation patterns of the associated emission intensities in the different ambient gases, which may arise from the use of ns and ps ablation lasers.

EXPERIMENTAL PROCEDURE

A description of the basic experimental setup used in this study is shown in Fig. 1. The chamber used is the same special cylindrical chamber of 115 mm inner diameter employed in our previous experiments[52–58] It was designed with several entry ports to allow for the control and monitoring of the specific conditions inside the chamber as needed by the experiment. For the current experiment, an additional ps laser (Nd:YAG, EKSPLA, model PL 2143, 1064 nm, 20 ps, maximum energy

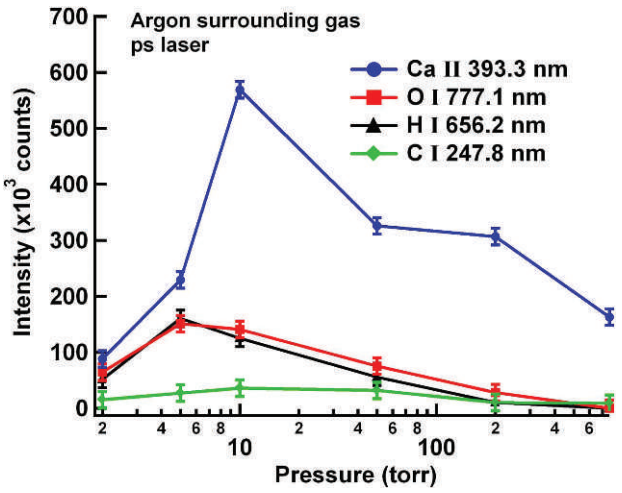

FIG. 3. Detailed illustration of H I 656.2 nm, O I 777.1 nm, Ca II 396.8 nm, and C I 247.8 nm emission intensity variations with respect to varying surrounding argon gas pressure. Picosecond YAG laser with energy of 7 mJ was focused onto agate sample.

of 30 mJ) was employed separately, and was operated in the Q-sw mode at 10 Hz repetition rate with the laser output energy fixed at a level as low as 7 mJ. The ps laser was chosen for the possibility of suppressing the unwanted heating effect due to the relatively long ns laser pulse of relatively large ablation energy, which may give rise to some unpredicted complications in the sample during the successive ablation processes. The ps laser can instead deliver the needed amount of power density with much smaller laser output energy with a much shorter pulse duration, and hence a much smaller crater size that is useful for microanalysis. For the purpose of comparative study, the ns Nd:YAG laser (Quanta-Ray, Lab Series, 1064 nm, 8 ns, maximum energy of 450 mJ) was also employed separately while operated in the same mode with the laser output energy fixed at 50 mJ. The laser beam was focused by a moveable lens of 120 mm focal length and directed perpendicularly onto different spots of the sample surface through a quartz window.

The agate sample employed as the main target in this experiment was cut into pellets of 10 × 10 mm cross-sectional area and 1 mm thickness. The sample chamber was evacuated using a vacuum pump to a pressure of 0.001 Torr. Subsequently, the chamber was heated up to 200 °C for 30 min to remove most of the residual surface water molecules. The high-purity buffer gas (Air Liquid, 5N) was introduced thereafter into the chamber until a pressure of 10 Torr was attained at a constant flow of 2 L/min. The gas pressure of 10 Torr and the chamber temperature of 200 °C were henceforth maintained throughout the experiment.

The plasma emission was detected by an optical multichannel analyzer (OMA) system (Andor iStar intensified CCD 1024 × 256 pixels), attached on its output side to a spectrograph (McPherson model 2061 with 1000 mm focal length f/8.6 Czerny Turner configuration), and connected to an optical fiber on the other side. The entrance end of the fiber was equipped in front of it with a movable local imaging module consisting of an entrance slit of 2.5 mm wide and a lens of 7.0 cm focal length. In the position shown in Fig. 1, each spot on the plasma along its axis of approximately 1 mm long was imaged onto the entrance end of the optical fiber with its output end connected to the OMA system. As the lens system can be freely moved along the direction of plasma expansion, it allows a spatial scan of the emission spectra over the entire length of the plasma. The spectral window of the detector has a width of 16 nm at 500 nm and the spectral resolution of the OMA system is 0.012 nm at 500 nm wavelength. The accumulated data of ten detected spectra from each irradiated spot were monitored on a screen and recorded to yield the averaged results presented in this report. The gate delay of the OMA system was set at 10 ns for the ps laser and 200 ns for the ns laser unless otherwise stated, while the same gate width of 50 μs was used in all cases except for time-resolved measurements for which much shorter gate widths were used, as noted later. The sample surface condition was constantly monitored during the repeated operations of laser irradiation by means of a stereo microscope (Mini-Stereo MDS-40, Nissho Optical Co., Ltd.) through a 50 mm quartz window installed parallel to the sample surface. The

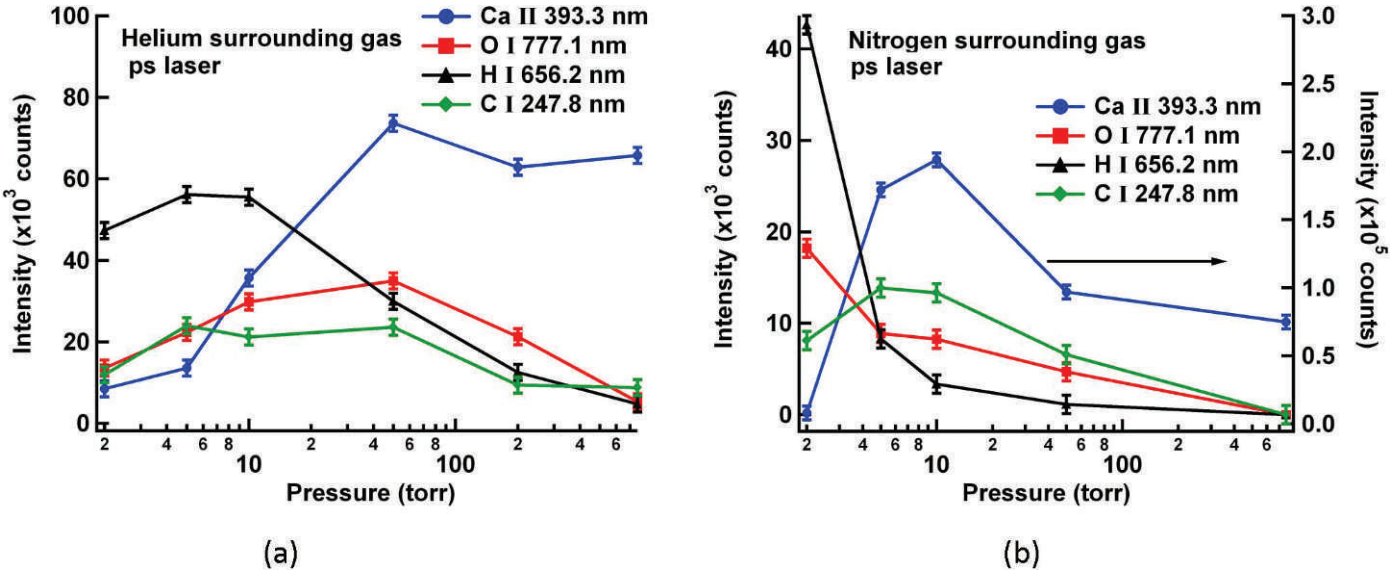

FIG. 4. Detailed illustration of H I 656.2 nm, O I 777.1 nm, Ca II 396.8 nm, and C I 247.8 nm emission intensities as functions of surrounding gas pressure in (**a**) helium and (**b**) nitrogen. Picosecond YAG laser with energy of 7 mJ was used for ablation of agate sample.

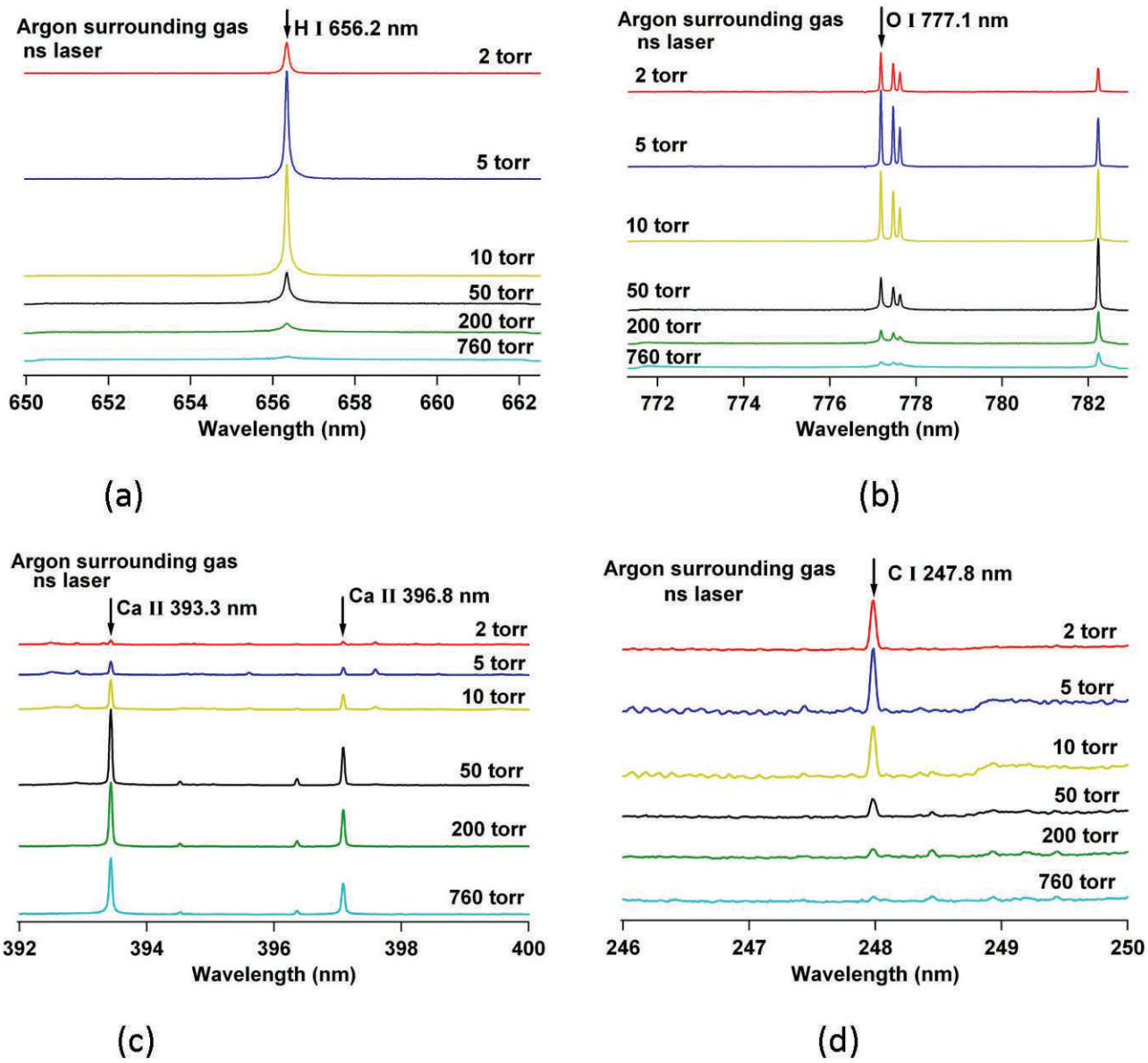

FIG. 5. Spatial and time-integrated emission spectra of (**a**) hydrogen, (**b**) oxygen, (**c**) calcium, and (**d**) carbon in various surrounding argon gas pressure when nanosecond laser of energy 50 mJ was used for ablation of agate sample.

working distance was fixed at 135 mm between the objective lens and the sample surface.

For the depth profile measurement, a preliminary experiment was carried out to determine the total number of laser shots it takes to "drill" through the sample of a known thickness. In the meantime, the stepwise increase of crater depth with each additional ablation laser shot was observed by the stereo microscope. The shot number can thus be used to provide a rough reference of the sample depth probed by each successive laser shot.

EXPERIMENTAL RESULTS AND DISCUSSION

Emission Characteristics in Different Gas Plasmas Induced by Different Lasers. Figure 2 shows the variations of spatial and time-integrated emission intensity of (a) hydrogen, (b) oxygen, (c) calcium, and (d) carbon with varying surrounding argon gas pressure when the agate sample is ablated by the ps laser energy of 7 mJ. Note that the weak neutral Ca emission line of 422.6 nm does not appear in the spectral range considered, while the ionic Ca II emission shown is stronger and hence more suitable for this study. The H and O emission intensities are seen to increase with the gas pressure up to their maxima at roughly the same pressure of 5 Torr, followed by a gradual decrease with increasing pressure, becoming negligible at 760 Torr. Meanwhile, the C emission with its relatively low intensity was nonetheless clearly detected and was relatively insensitive to pressure change. Remarkably, the ionic Ca emission intensity shown in Fig. 2c exhibits a steep rise to its maximum at 10 Torr, followed by an equally fast decline with increasing pressure of up to 50 Torr, and continues to decrease more gradually with a further increase of pressure and remains finite at 760 Torr. An overall comparison of those pressure-dependent behaviors is illustrated more clearly in Fig. 3. One notes that in spite of the widely different patterns of intensity variation, all the maximum

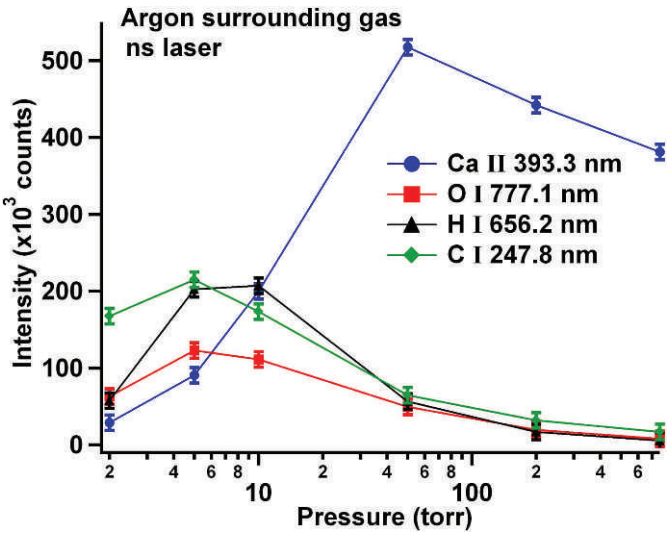

FIG. 6. Detailed illustration of H I 656.2 nm, O I 777.1 nm, Ca II 396.8 nm, and C I 247.8 nm emission intensities as functions of surrounding argon gas pressure. Nanosecond YAG laser with energy of 50 mJ was employed in this measurement.

emission intensities observed in Ar surrounding gas occur in the relatively narrow range of gas pressure from 5 to 10 Torr.

Figure 4 shows the pressure-dependent intensity variations of the same emission lines in different surrounding gases of (a) He and (b) N_2, measured with exactly the same experimental condition. Comparing Figs. 4a and 4b clearly shows the different pressure effects on different emission lines observed in different ambient gases. For instance, relatively little qualitative differences are displayed in the pressure-dependent effects of the O and C emission lines, but drastic changes of behavior are observed between the H and Ca emission intensities. It is noteworthy from Figs. 3 and 4 that H emission intensities are generally more sustainable at higher pressure in the case of He surrounding gas, although the Ar surrounding gas appears to produce generally higher emission intensities except for the C emission.

In view of the existing common use of ns laser in practical spectrochemical analysis, it is desirable to investigate the possibly different pressure-dependent effects on those emission lines in ns laser induced plasma. To this end, the experiment was repeated by employing the ns laser operated in exactly the same mode with nonetheless much higher energy of 50 mJ. The resulted spectra are presented in Fig. 5 for the same pressure variations. A complete illustration of the pressure-dependent effects is presented in Fig. 6. It can be seen that the H, O, and C emission intensities rise to their individual maximum at the same gas pressure of about 5 Torr, before decreasing with increasing pressure, and eventually vanish at 760 Torr. Meanwhile, the Ca II emission intensity exhibits a sharp increase to remarkably higher maximum at much greater pressure of 50 Torr, followed by a relatively slow decline with increased pressure. One notes that the behaviors of the C and Ca II emission lines are in clear contrast to those found in Fig. 3, and generally the pressure effect varies more sensitively with different emission lines in the plasma induced by ns laser.

Repeating the same experiment in He and N_2 surrounding gases yielded the pressure-dependent intensity profiles presented in Fig. 7 for (a) He and (b) N gases. These intensity profiles are seen to vary more widely in their pressure effects compared to those found in Fig. 4. We note further from Figs. 3, 4, 5, and 7 that H and Ca emission intensities are generally higher in Ar surrounding gas at low pressures around 5 Torr, while the ps laser generally produces at least comparable if not higher emission intensities in the low-pressure Ar gas, which is the reason for its choice in the following experiment.

Shock Wave Excitation in ps Laser-Induced Plasma. In a previous work using ns laser,[54] part of the H atoms were found to be ejected at very high initial speed, leaving behind it the heavier ablated atoms of the host elements, which are responsible for the formation of a thermal shock wave and the shock excitation of those atoms right behind the shock front.[54] As the plasma expands at the shock wave speed, the

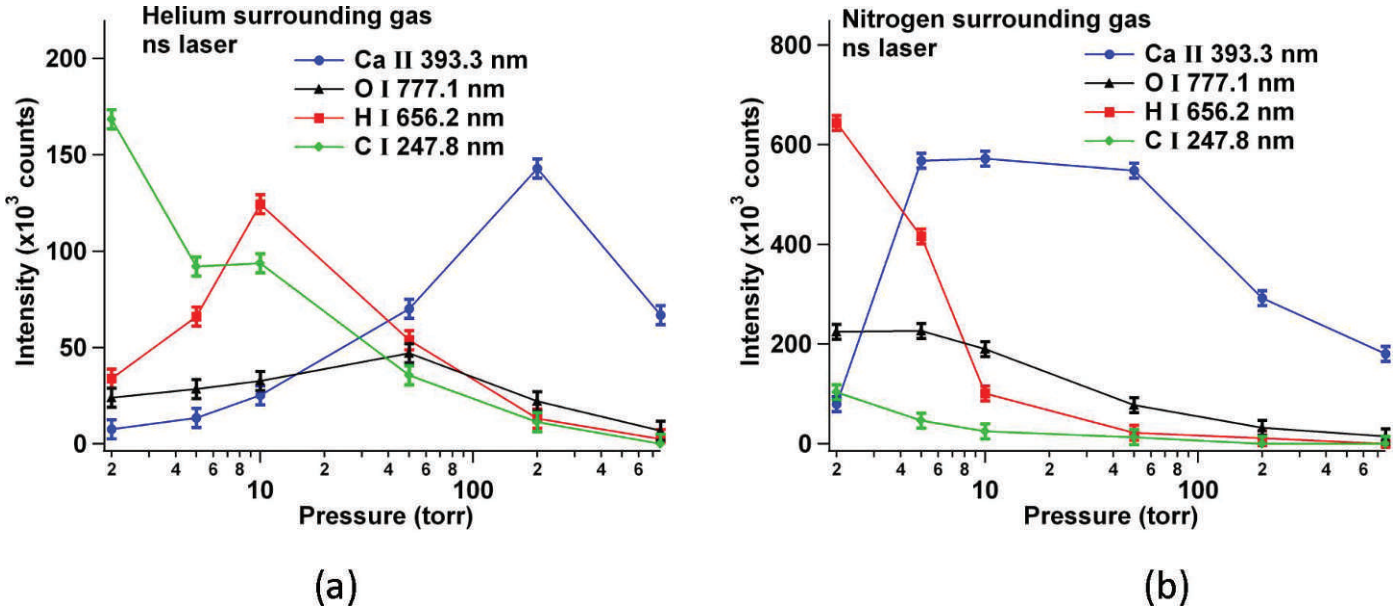

FIG. 7. Detailed illustration of H I 656.2 nm, O I 777.1 nm, Ca II 396.8 nm, and C I 247.8 nm emission intensities as functions of surrounding gas pressure in (**a**) helium and (**b**) nitrogen. Nanosecond YAG laser with energy of 50 mJ was used for ablation of agate sample.

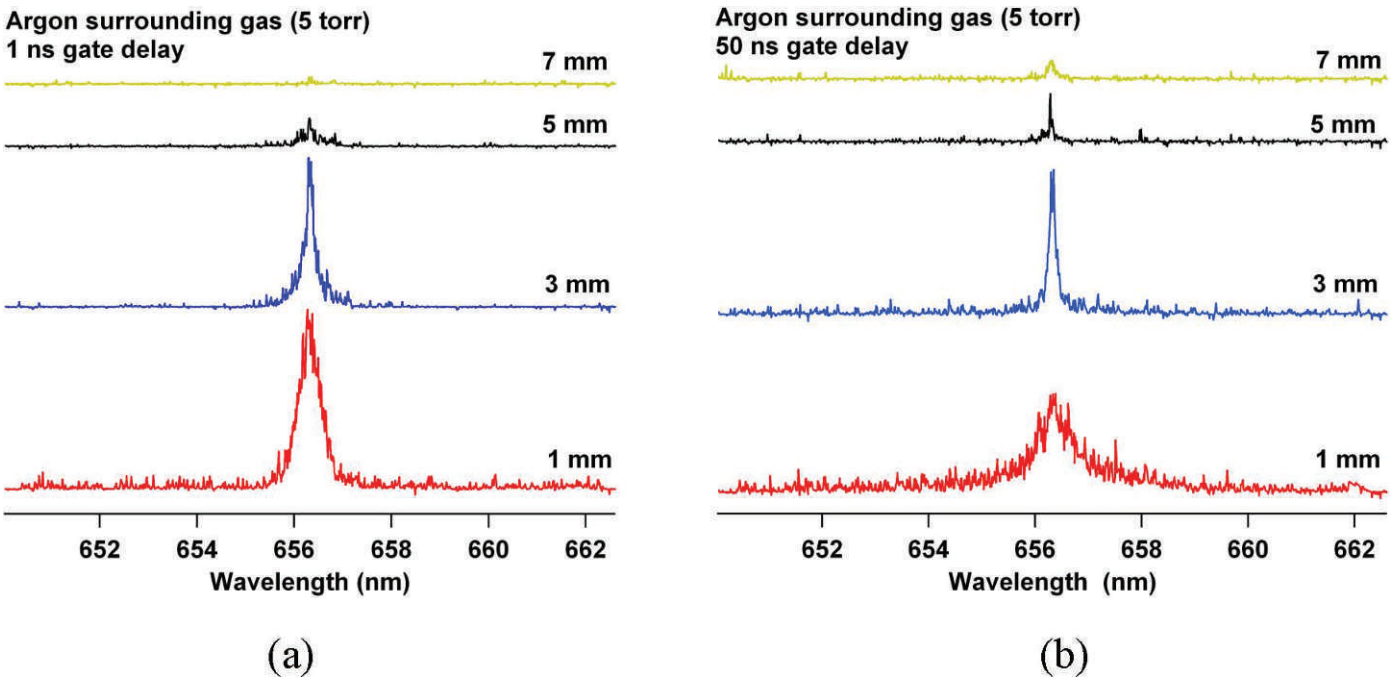

FIG. 8. H I 656.2 nm emission spectra detected from different plasma positions of different distances from the sample surface, with gate width of 50 μs and different gate delays of the OMA system (**a**) 1 ns and (**b**) 50 ns in surrounding argon gas at 5 Torr. The ps YAG laser was used for the target ablation at an energy of 7 mJ.

plasma shock front will leave the cluster of atoms further behind it, thereby reducing the excitation efficiency leading to decreasing emission intensity over the long plasma cooling process. The low H emission intensity observed at the higher gas pressure was explained on the basis of the shock wave model as due to the time mismatch between the shock wave formation and the passage of the fast-moving H atoms. It is important to examine whether a different dynamical process and the related emission characteristics would arise in ps laser-induced plasma. For this purpose, an experiment with ps laser was carried out using the imaging technique explained earlier. The detected H emission lines from varying plasma positions are plotted in Fig. 8 for 5 Torr Ar gas pressure and gate delay of (a) 1 ns and (b) 50 ns. It is seen that a small but clearly visible H emission already appears in 1 ns at relatively large distances of 5 and 7 mm from the sample surface. In view of the relatively large OMA gate width, the distinct abruptly reduced signals at those two distances apparently indicate the much shorter duration of the emission compared to those observed at closer distances. As explained above, those signals are clearly not due to the shock excitation. Instead, it more likely resulted from excitation due to the collision between the Ar atoms and the few fastest-moving H atoms that have passed through the plasma prior to the formation of the thermal shock wave. On the other hand, the much larger emission signals occurring at 3 and 1 mm exhibit broader spectral lines with closer position to the target. These are characteristics of an emission induced by the hot plasma shock wave, which lasts

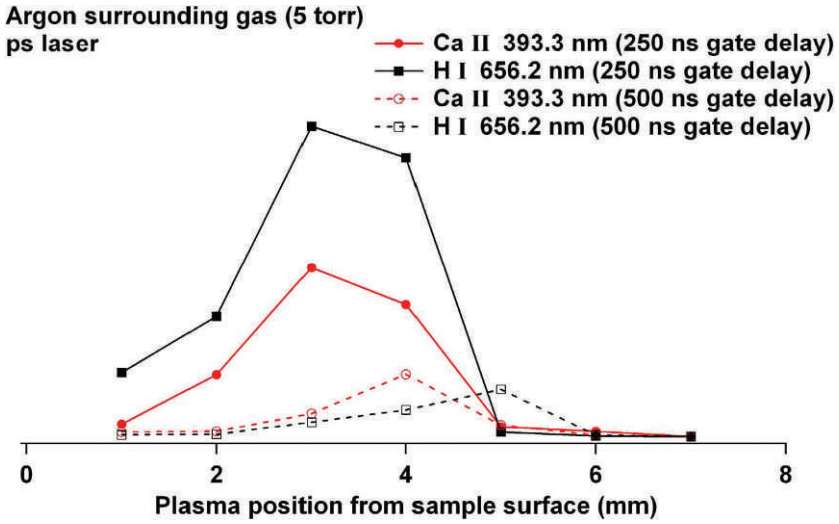

FIG. 9. Profiles of spatial variations of H I 656.2 nm and Ca II 396.8 nm emission intensities measured with OMA gate width of 10 ns at different OMA gate delay (**a**) 250 ns and (**b**) 500 ns. Picosecond YAG laser with energy of 7 mJ was used for ablation of agate sample in surrounding argon gas at 5 Torr.

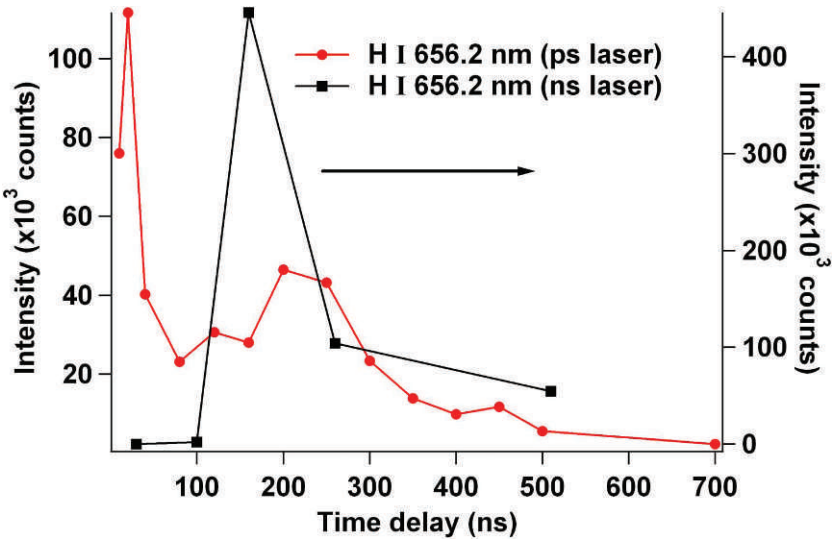

FIG. 10. Time profiles of total emission intensity of H I 656.2 nm from agate sample in argon surrounding gas of 5 Torr. Nanosecond YAG laser of 50 mJ energy and picosecond YAG laser of 7 mJ energy were employed in separate measurements.

longer due to the long plasma cooling stage following the short shock excitation stage described above. In addition, the stronger Stark broadening is associated with the higher charge particle density in the plasma closer to the sample surface. Interestingly, the occurrence of a collision-induced emission observed at 7 mm within 1 ns allows the estimation of the initial highest speed of the H atom, which is about 7000 km/s. The result obtained with 50 ns gate delay when the shock wave excitation is fully operative is presented in Fig. 8b. It shows that H emission at 1 mm is most severely broadened as expected. Further away at 3, 5, and 7 mm from the sample surface, the hot plasma is already expanded, leading to lesser charge density and lower temperature and hence correspondingly sharper emission lines.

Further study of the dynamics of the H and other host atoms during the ablation process is carried out by measuring the time-resolved spatial distribution of H and Ca emission intensities with OMA gate width of 1 μs and for different gate delays of 250 and 500 ns separately. The results are given in Fig. 9. It shows basically the same rise patterns of early spatial intensity variations of both emission lines measured with 250 ns gate delay, and both intensities finally drop to zero at 5 mm. This common feature is typical of shock wave-induced emission of the ablated atoms at the initial stage, regardless of their mass differences.[54] With increasing time, however, the shock excitation is expected be less effective due to widening distance between the shock front and the cluster of heavier ablated atoms left behind, resulting in much lower emission intensities detected with 500 ns gate delay, as shown in the figure.

Finally, a study of the transient H emission process taking place during the plasma expansion was performed by measuring the time profiles of the spatially integrated intensities in Ar plasmas separately generated by ns and ps lasers. The result presented in Fig. 10 shows, in the case using the ns laser, a steep rise of the H emission intensity up to its

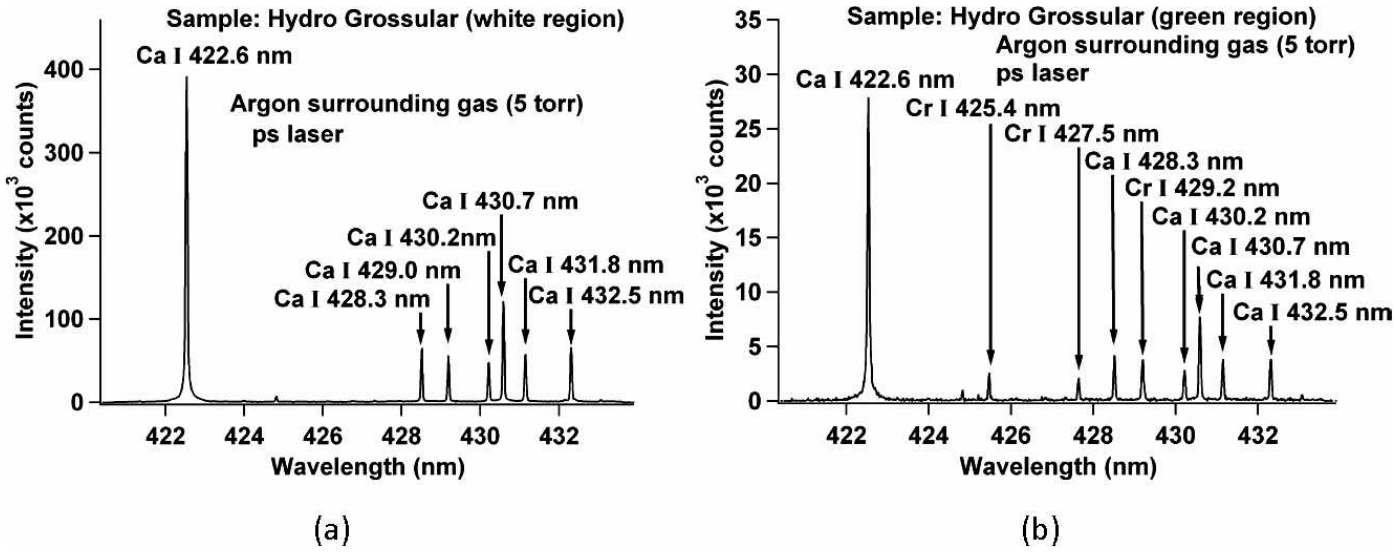

FIG. 11. Emission spectrum from hydrogrossular sample in surrounding argon gas at 5 Torr detected from the (**a**) white region and (**b**) green region with ps YAG laser of energy 7 mJ.

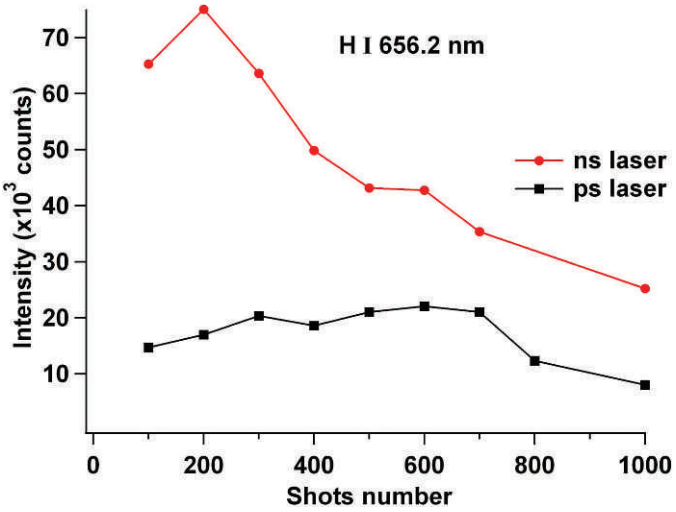

FIG. 12. Intensity depth profiles of H I 656.2 nm emission from agate sample using ns (50 mJ) and ps (7 mJ) YAG laser separately in surrounding argon pressure of 5 Torr.

maximum at 150 ns before its equally fast downturn, followed by continued decrease at much lower pace, in good agreement with the proposed scenario consisting of short excitation and long cooling stages in the shock wave model.[59] In the case of the ps laser, the intensity time profile apparently consists of two components. The first one exhibits an even sharper spike in the early stage of the laser irradiation. As noted in connection with Fig. 8a, the transient nature of this spike is indicative of its origin in the excitation induced by collision between the Ar atoms in the surrounding gas and the ablated H atoms moving at very high initial speed as estimated earlier from Fig. 8a. On the other hand the second component is characteristic of shock wave-induced emission from a small part of the slower H atoms. This part of the time profile shows a rapid initial increase up to its maximum in 200 ns and the subsequent decrease at a lower pace followed by a long tail. This is basically similar to that observed in the case employing ns laser and in good agreement with the shock wave model.[59] This result has thus demonstrated the occurrence of a new transient feature at the very early stage in addition to the later intensity time profile that exhibits the shock wave-induced emission characteristics in the plasma generated by the ps laser, resembling the same basic feature shown in Fig. 8a for ns laser-induced plasma emission.

Demonstration of Favorable Applications with ps Laser. In addition to the advantages of the ps laser mentioned in the experimental procedure, the demonstrated experimental results are now verified by their application to spectrochemical analysis of a hydrogrossular stone sample (main composition: 35% SiO_2, 19.87% Al_2O_3, 0.61% Fe_2O_3, 0.85% FeO, 37.4% CaO, 2.07% MgO, and 4.65% H_2O). The stone color is basically green with some minor white spots. The resulting spectra presented in Fig. 11, as obtained from different white and green areas of the stone, clearly show that more chromium emission lines are detected from the green area. Further, a study was performed on its possible application to determining the intensity variation with increasing crater depth by conducting a depth profile measurement also carried out on the agate sample of known thickness. The emission intensity of H was measured stepwise, with every step consisting of data detected from 100 successive shots, which were then averaged to produce the result plotted in Fig. 12. As the repeated laser shots directed onto the same sample spot were expected to deepen the crater accordingly, the intensity variation with each additional 100 shots may effectively represent the intensity depth profile of the associated emission. Plotted in Fig. 12 are the variations of H emission intensity with each of the additional 100 successive shots measured separately with the ns and ps lasers. It is seen that the intensity remains more or less constant over the entire process of up to 700 ps laser shots, in good agreement with the well-known homogeneity of the H impurity distribution in the sample. On the other hand, the result obtained with the ns laser shows a large initial increase in the intensity and a continued decrease thereafter, contrary to the actual distribution of H impurity in the sample. Obviously, the intensity profile obtained with ps laser provides a more faithful representation of the H impurity distribution inside the sample. Presumably, this is due to the much smaller heating effect produced by the ps laser. It has thus further demonstrated the advantage of ps laser over the ns laser. A microscopic measurement conducted on the craters produced after 700 laser shots of ns and ps lasers yielded crater diameters of 1 mm for ns laser and 0.15 mm for ps laser, while producing roughly the same crater depth of 1.5 mm for both.

CONCLUSION

This experiment shows the different pressure-dependent effects of the emission intensities of H, O, C, and Ca from agate sample, which further vary with the different surrounding gases used and different ablation lasers employed. It is found that consistently better emission qualities are obtained by using the ps laser in Ar surrounding gas. The detailed measurements of spatial distributions and time profiles of emission intensities further reveal similar features of the shock wave excitation-induced emission in both plasmas generated either by ns or ps lasers, while the ps laser-induced plasma does exhibit an additional early and transient H emission spike due to the collision induced excitation. Finally, the excellent quality of its application to spectrochemical analysis is demonstrated by the emission spectra of hydrogrossular sample. Further application to depth profiling of H impurity distribution also clearly shows a more faithful result obtained by employing the ps laser.

ACKNOWLEDGMENTS

Part of this work was supported by Third World Academy of Sciences (TWAS) Italy, through a Basic Research Grant in Physics, Contract No. 03-109RG/PHYS/AS. Also part of this work was supported by Ms. Steffi Kurniawan.

1. F. Brech, L. Cross. "Optical Micro Emission Stimulated by a Ruby Laser". Appl. Spectrosc. 1962. 16: 59.
2. A.W. Miziolek, V. Palleschi, I. Schechter. Laser-Induced Breakdown Spectroscopy (LIBS) Fundamentals and Applications. Cambridge, UK: Cambridge University Press, 2006.
3. L. Moenke-Blankenburg. Laser Microanalysis. New York, USA: Wiley, 1989.
4. Y. Talmi, H.P. Sieper, L. Moenke-Blankenburg. "Laser-Microprobe Elemental Determinations with an Optical Multichannel Detection System". Anal. Chim. Acta. 1981. 127(6): 71-85.
5. H.J. Hakkanen, J.E.I. Korppi-Tommola. "UV-Laser Plasma Study of Elemental Distributions of Paper Coating". Appl. Spectrosc. 1995. 49(12): 1721-1728.
6. H. Wiggenhauser, D. Schaurich, G. Wilsch. "LIBS for Non-Destructive Testing of Element Distributions on Surface". NDT&E Int. 1998. 31(4): 307-313.
7. D. Romero, J.M. Fernandez-Romero, J.J. Laserna. "Distribution of Metal Impurities in Silicon Wafers Using Imaging-Mode Multi-Elemental Laser-

Induced Breakdown Spectrometry". J. Anal. Atom. Spectrom. 1999. 14(2): 199-204.
8. J.M. Vadillo, S. Palanco, M.D. Romero, J.J. Laserna. "Applications of Laser-Induced Breakdown Spectrometry (LIBS) in Surface Analysis". J. Anal. Chem. 1996. 355(7–8): 909-912.
9. C. Fabre, M.C. Boiron, J. Dubessy, A. Moissette. "Determination of Ions in Individual Fluid Inclusions by Laser Ablation Optical Emission Spectroscopy: Development and Applications to Natural Fluid Inclusions". J. Anal. Atom. Spectrom. 1999. 14(6): 913-922.
10. J.D. Winefordner, I.B. Gornushkin, T. Correll, E. Gibb, B.W. Smith, N. Omenetto. "Comparing Several Atomic Spectrometric Methods to the Super Stars: Special Emphasis on Laser Induced Breakdown Spectrometry, LIBS, a Future Super Star". Anal. Atom. Spectrom. 2004. 19(9): 1061-1083.
11. I. Zergioti, M. Stuke. "Short Pulse UV Laser Ablation of Solid and Liquid Gallium". Appl. Phys. A. 1998. 67(4): 391-395.
12. B.N. Chirchkov, C. Momma, S. Nolte, F. von Alvensleben, A. Tunnermann. "Femtosecond, Picosecond, and Nanosecond Laser Ablation of Solids". Appl. Phys. A. 1996. 63(2): 109-115.
13. R.E. Russo, X.L. Mao, S.S. Mao. "The Physics of Laser Ablation in Microchemical Analysis". Anal. Chem. 2002. 74(3): 70A-77A.
14. S.M. Angel, D.N. Stratis, K.L. Eland, T. Lai, M.A. Berg, D.M. Gold. "LIBS Using Dual- and Ultra-Short Laser Pulses". Fresenius' J. Anal. Chem. 2001. 369(3–4): 320-327.
15. A. Semerok, B. Salle, J.-F. Wagner, G. Petite. "Femtosecond, Picosecond, and Nanosecond Laser Microablation: Laser Plasma and Crater Investigation". Las. Part. Beams. 2002. 20(1): 67-72.
16. L. Xu, V. Bulatov, V.V. Gridin, I. Schechter. "Absolute Analysis of Particulate Material by Laser-Induced Breakdown Spectroscopy". Anal. Chem. 1997. 69(11): 2103-2108.
17. R. Wisbrun, I. Schechter, R. Niessner, H. Schroder, K. Kompa. "Detector For Trace Elemental Analysis of Solid Environmental Samples by Laser Plasma Spectroscopy". Anal. Chem. 1994. 66(18): 2964-2975.
18. M. Sabsabi, P. Cielo. "Quantitative Analysis of Aluminum Alloys by Laser-Induced Breakdown Spectroscopy and Plasma Characterization". Appl. Spectrosc. 1995. 49(4): 499-507.
19. P. Fichet, P. Mauchien, J.F. Wagner, C. Moulin. "Quantitative Elemental Determination in Water and Oil by Laser-Induced Breakdown Spectroscopy". Anal. Chim. Acta. 2001. 429(2): 269-278.
20. A. Ciucci, M. Corsi, V. Palleschi, S. Rastelli, A. Salvetti, E. Tognoni. "New Procedure for Quantitative Elemental Analysis by Laser-Induced Plasma Spectroscopy". Appl. Spectrosc. 1999. 53(8): 960-964.
21. D. Anglos, V. Zafiropulos, K. Melessanaki, M.J. Gresalfi, J.C. Miller. "Laser-Induced Breakdown Spectroscopy for the Analysis of 150-year Old Daguerreotypes". Appl. Spectrosc. 2002. 56(4): 423-430.
22. M.S. Barger, W.B. White. The Daguerreotype, Nineteenth-century Technology and Modern Science. Baltimore: The John Hopkins University Press, 1991.
23. D. Romero, J.J. Laserna. "Surface and Tomographic Distribution of Carbon Impurities in Photonic-Grade Silicon Using Laser-Induced Breakdown Spectrometry". J. Anal. Atom. Spectrom. 1998. 13(6): 557-560.
24. D. Anglos. "Laser-Induced Breakdown Spectroscopy in Art and Archaeology". Appl. Spectrosc. 2001. 55(6): 186A.
25. M. Kraushaar, R. Noll, H.U. Schmitz. "Multi-Elemental Analysis of Slag from Steel Production Using Laser-Induced Breakdown Spectroscopy (LIBS)". In: International Meeting on Chemical Engineering, Environmental Protection and Biotechnology, ACHEMA 2000, Laboratory and Analysis Accreditation, Certification and QM. 2000. Pp. 117-119.
26. V. Sturm, L. Peter, R. Noll. "Steel Analysis with Laser-induced Breakdown Spectrometry in the Vacuum Ultraviolet". Appl. Spectrosc. 2000. 54(9): 1275-1278.
27. V. Palleschi, G. Cristoforetti, M. Corsi, M. Giuffrida, M. Hidalgo, D. Iriarte, S. Legnaioli, A. Salvetti, E. Tognoni. "Micro-LIBS and Micro-Raman Spectroscopy Analysis". LIBS 2002 Technical Digest. Conference on Laser Induced Plasma Spectroscopy and Applications, Orlando, FL; September 25, 2002. Pp 172-174.
28. A. Uhl, K. Loebe, L. Kreuchwig. "Fast Analysis of Wood Preservers Using Laser-Induced Breakdown Spectroscopy". Spectrochim. Acta. 2001. B56(6): 795-806.
29. R. Sattmann, I. Monch, H. Krause, R. Hall, S. Couris, A. Hatziapostolou, A. Mauromanolakis, C. Fotakis, E. Larrauri, R. Miguel. "Laser-Induced Breakdown Spectroscopy for Polymer Identification". Appl. Spectrosc. 1998. 52(3): 456-462.
30. J. Gruber, J. Heitz, H. Strasser, D. Bauerle, N. Ramaseder. "Rapid In Situ Analysis of Liquid Steel by Laser-Induced Breakdown Spectroscopy". Spectrochim. Acta. 2001. B56(6): 685-693.
31. R.E. Neuhauser, U. Panne, R. Niessner, G.A. Petrucci, P. Cavalli, N. Omenetto. "On-line and in Situ Detection of Lead Aerosol by Plasma Spectroscopy and Laser-Excited Atomic Fluorescence Spectroscopy". Anal. Chim. Acta. 1997. 346(1): 37-48.
32. O. Samek, D.C.S. Beddows, J. Kaiser, S. Kukhlevsky, L. Miroslav, H.H. Telle, J.A. Whitehouse. "The Application of Laser–Induced Breakdown Spectroscopy to in Situ Analysis of Liquid Samples". Opt. Eng. 2000. 39(8): 2248-2262.
33. Y. Ito, O. Ueki, S. Nakamura. "Determination of Colloidal Iron in Water by Laser-Induced Breakdown Spectroscopy". Anal. Chim. Acta. 1995. 299(3): 401-405.
34. H.A. Archontaki, S.R. Crouch. "Evaluation of an Isolated Droplet Sample Introduction System for Laser-Induced Breakdown Spectroscopy". Appl. Spectrosc. 1988. 42(5): 741-746.
35. F.Y. Yueh, R.C. Sharma, J.P. Singh, H. Zhang. "Evaluation of the Potential of Laser-Induced Breakdown Spectroscopy for Detection of Trace Element in Liquid". J. Air Waste Manage. Assoc. 2002. 52(11): 1307-1315.
36. M.O. Al-Jeffery, H.H. Telle. "LIBS and LIFS for Rapid Detection of Rb Traces in Blood". Proc. SPIE, Optical Biopsy IV. 2002. 4613: 152-161.
37. T. Prohaska, C. Stadlbauer, R. Wimmer, G. Stingeder, C. Latkaczy, E. Hoffmann, E. Stephanowitz. "Investigation of Element Variability in Tree Rings of Young Norway Spruce by Laser-Ablation-ICPMS". Sci. Total Environ. 1998. 219(1): 29-39.
38. M.H. Niemz. "Investigation and Spectral Analysis of the Plasma-Induced Ablation Mechanism of Dental Hydroxyapatite". Appl. Phys. B. 1994. 58(4): 273-281.
39. I.G. Pallikaris, H.S. Ginis, G.A. Kounis, D. Anglos, T.G. Papazoglou, L.P. Naomidis. "Corneal Hydration Monitored by Laser-induced Breakdown Spectroscopy". J. Refractive. Surg. 1998. 14(6): 655-660.
40. G.P. Sighinolfi, S. Sartono, Y.G. Artoli. "Chemical and Mineralogical Studies on Hominid Remains from Sangiran Central Java (Indonesia)". J. Hum. Evol. 1993. 24(1): 57-68.
41. R.K. Chang, J.H. Eickmans, W.F. Hsieh, C.F. Wood, J.Z. Zhang, J.B. Zhang. "Laser-Induced Breakdown in Large Transparent Water Droplets". Appl. Opt. 1988. 27(12): 2377-2385.
42. L.J. Radziemski, T.R. Loree, D.A. Cremers, N.M. Hoffman. "Time-Resolved Laser-Induced Breakdown Spectrometry of Aerosols". Anal. Chem. 1983. 55(8): 1246-1252.
43. D.W. Hahn, M.M. Lunden. "Detection and Analysis of Aerosol Particles by Laser-Induced Breakdown Spectroscopy". Aerosol Sci. Technol. 2000. 33: 30-48.
44. Y.L. Chen, J.W.L. Lewis, C. Parigger. "Spatial and Temporal Profiles of Pulsed Laser-Induced Air Plasma Emissions". J. Quant. Spectrosc. Radiat. 2001. 67(2): 91-103.
45. S. Yalcin, D.R. Crosley, G.P. Smith, G.W. Faris. "Influence of Ambient Conditions on the Laser Air Spark". Appl. Phys. B. 1999. 68(1): 121-130.
46. N. Konjevic. "Plasma Broadening and Shifting of Non-Hydrogenic Spectral Lines: Present Status and Applications". Phys. Reports. 1999. 316(6): 399-403.
47. R. Zikic, M.A. Gigosos, M. Ivkovic, M.A. Gonzalez, N. Konjevic. "A Program for the Evaluation of Electron Number Density from Experimental Hydrogen Balmer Beta Line Profiles". Spectrochim. Acta. 2002. B57(5): 987-995.
48. N. Idris, S. Terai, T.J. Lie, K.H. Kurniawan, T. Kobayashi, T. Maruyama, K. Kagawa. "Hydrogen Emission Induced by TEA CO_2 Laser Bombardment on Solid Samples at Low Pressure and its Analytical Application". Appl. Spectrosc. 2005. 59(1): 115-120.
49. N. Idris, K.H. Kurniawan, T.J. Lie, M. Pardede, H. Suyanto, R. Hedwig, T. Kobayashi, K. Kagawa, T. Maruyama. "Characteristics of Hydrogen Emission in Laser Plasma Induced by Focusing Fundamental Q-sw YAG Laser on Solid Samples". Jpn. J. Appl. Phys. 2004. 43: 4221-4226.
50. K.H. Kurniawan, T.J. Lie, N. Idris, T. Kobayashi, T. Maruyama, H. Suyanto, K. Kagawa, M.O. Tjia. "Hydrogen Emission by YAG Laser-Induced Shock Wave Plasma and its Application to the Quantitative Analysis of Zircaloy". J. Appl. Phys. 2004. 96(3): 1301-1309.
51. T.J. Lie, K.H. Kurniawan, D.P. Kurniawan, M. Pardede, M.M. Suliyanti, A. Khumaeni, S.A. Natiq, S.N. Abdulmadjid, Y.I. Lee, K. Kagawa, N. Idris, M.O. Tjia. "Elemental Analysis of Bead Samples Using a Laser-Induced Plasma at Low Pressure". Spectrochim. Acta. 2006. B61(1): 104-112.
52. K.H. Kurniawan, M. Pardede, R. Hedwig, Z.S. Lie, T.J. Lie, D.P. Kurniawan, M. Ramli, K. Fukumoto, H. Niki, S.N. Abdulmadjid, N. Idris, T. Maruyama, K. Kagawa, M.O. Tjia. "Quantitative Hydrogen Analysis of Zircaloy-4 Using Low-Pressure Laser Plasma Technique". Anal. Chem. 2007. 79(7): 2703-2707.
53. S.N. Abdulmadjid, Z.S. Lie, H. Niki, M. Pardede, R. Hedwig, T.J. Lie, E. Jobiliong, K.H. Kurniawan, K. Fukumoto, K. Kagawa, M.O. Tjia.

"Quantitative Deuterium Analysis of Titanium Samples in UV Laser-Induced Low-Pressure Helium Plasma". Appl. Spectrosc. 2010. 64(4): 365-369.
54. K.H. Kurniawan, K. Kagawa. "Hydrogen and Deuterium Analysis Using Laser-Induced Plasma Spectroscopy". Appl. Spectrosc. Rev. 2006. 41(2): 99-130.
55. M. Pardede, R. Hedwig, M.M. Suliyanti, Z.S. Lie, T.J. Lie, D.P. Kurniawan, K.H. Kurniawan, M. Ramli, K. Fukumoto, H. Niki, S.N. Abdulmadjid, N. Idris, T. Maruyama, K. Kagawa, M.O. Tjia. "Comparative Study of Laser-Induced Plasma Emission of Hydrogen from Zircaloy-2 Samples in Atmospheric and Low Pressure Ambient Helium Gas". Appl. Phys. B. 2007. 89(2-3): 291-298.
56. M. Ramli, K. Fukumoto, H. Niki, S.N. Abdulmadjid, N. Idris, T. Maruyama, K. Kagawa, M.O. Tjia, M. Pardede, K.H. Kurniawan, R. Hedwig, Z.S. Lie, T.J. Lie, D.P. Kurniawan. "Quantitative Hydrogen Analysis of Zircaloy-4 in Laser-Induced Breakdown Spectroscopy with Ambient Helium Gas". Appl. Opt. 2007. 46(34): 8298-8304.
57. M. Munadi;, R.H. Pardede, M.M. Suliyanti, T.J. Lie, Z.S. Lie, K.H. Kurniawan, K. Kagawa, M. Ramli, K. Fukumoto, T. Maruyama, M.O. Tjia. "Study of Hydrogen and Deuterium Emission Characteristics in Laser-Induced Low Pressure Helium Plasma for the Suppression of Surface Water Contamination". Anal. Chem. 2008. 80(4): 1240-1246.
58. R. Hedwig, Z.S. Lie, K.H. Kurniawan, A.N. Chumakov, K. Kagawa, M.O. Tjia. "Toward Quantitative Deuterium Analysis with Laser-Induced Breakdown Spectroscopy Using Atmospheric-pressure Helium Gas". J. Appl. Phys. 2010. 107(2): 023301 1-5.
59. W.S. Budi, H. Suyanto, K.H. Kurniawan, M.O. Tjia, K. Kagawa. "Shock Excitation and Cooling Stage in the Laser Plasma Induced by a Q-switched Nd: YAG Laser at Low Pressures". Appl. Spectrosc. 1999. 53(6): 719-730.